JIPK. Volume 17 No 2 June 2025
Sinta 1 (Decree No: 158/E/KPT/2021)
e-ISSN:2528-0759; p-ISSN:2085-5842
Available online at https://e-journal.unair.ac.id/JIPK

JIPK
(JURNAL ILMIAH PERIKANAN DAN KELAUTAN)
Scientific Journal of Fisheries and Marine

Research Article

Shoreline Change Detection Using DSAS: Case Study in PT IWIP Mining Industrial Area, North Maluku Province, Indonesia

Nurhalis Wahidin[1*], Adi Noman Susanto[1], Irham[1], Zulhan Arifin Harahap[2], Salnuddin[2], and Muhammad Aris[3]

[1]Department of Aquatic Resources Management, Faculty of Fisheries and Marine Science, Universitas Khairun, Ternate. Indonesia
[2]Department of Marine Science, Faculty of Fisheries and Marine Science, Universitas Khairun, Ternate. Indonesia
[3]Department of Aquaculture, Faculty of Fisheries and Marine Science, Universitas Khairun, Ternate. Indonesia

OPEN ACCESS

ARTICLE INFO

Received: Oct 14, 2024
Accepted: May 18, 2025
Published: May 20, 2025
Available online: May 25, 2025

*) Corresponding author:
E-mail: nurhalis@unkhair.ac.id

Keywords:
Shoreline changes
Industrial area
Landsat
Abrasion
Accretion

Abstract

The development of industrial estate infrastructure in coastal areas causes significant changes in coastal morphology. Despite extensive infrastructure development in coastal zones, limited empirical data exists on the shoreline dynamics of newly established industrial estates, particularly in Eastern Indonesia, thus highlighting the urgency of this study. This study investigates coastal morphology changes in the PT Indonesia Weda Bay Industrial Park (IWIP) industrial area over five years using Landsat 8 OLI level 2A satellite imagery and geospatial analysis. Shoreline extraction was performed using the Normalized Difference Water Index (NDWI) algorithm and analyzed with the Digital Shoreline Analysis System (DSAS) applying the Net Shoreline Movement (NSM), End Point Rate (EPR), and Linear Regression Rate (LRR) methods. The findings show that from 2018 to 2023, the shoreline in the PT IWIP area predominantly experienced accretion. The highest rate of shoreline accretion occurred in industrial zone, with a maximum of 147.58 m/year and an average of 36.56 m/year, while residential zones in the eastern and western regions experienced moderate abrasion, with a maximum of 12.32 m/year and an average of 4.11 m/year. Categorization followed standard DSAS criteria, where shoreline changes between 10–30 m/year were considered moderate, and changes above 30 m/year were classified as very high. Measurement accuracy was validated using high-resolution Google Earth imagery and Landsat metadata, ensuring positional accuracy within ±30 meters. These results highlight the rapid and spatially varied shoreline changes driven by industrial activities, emphasizing the importance of remote sensing in monitoring and managing coastal development impacts.

Cite this as: Wahidin, N., Susanto, A. N., Irham, Harahap, Z. A., Salnuddin, & Aris, M. (2025). Shoreline Change Detection Using DSAS: Case Study in PT IWIP Mining Industrial Area, North Maluku Province, Indonesia. *Jurnal Ilmiah Perikanan dan Kelautan,* 17(2):470-484. https://doi.org/10.20473/jipk.v17i2.64271

1. Introduction

The PT Indonesia Weda Bay Industrial Park (IWIP) is an integrated Industrial Estate for heavy metal processing located in Lelilef Village, Weda District, Central Halmahera Regency, in Indonesia's North Maluku Province. IWIP was designated as a National Strategic Projects under Presidential Regulation No. 109/2020, highlighting its national importance in accelerating downstream mining activities concerning the Third Amendment to Presidential Regulation No. 3/2016 for the Acceleration of the Implementation of National Strategic Projects. The industrial area within the IWIP, which was established on August 30, 2018 is also a National Priority Project based on PERPRES No. 18, concerning the National Medium-Term Development Plan for 2020-2024. Since the establishment of the industrial area, various infrastructures have been built in its coastal areas that have dramatically changed the morphology of the surrounding coast. Construction in the IWIP industrial area included reclaiming coastal areas and converting important coastal resources such as coral reefs and mangrove forests into port facilities.

Examining the trends of shoreline change over time is one of the best methods to track the combined effects of human activity and natural processes on shorelines. (Al-Hatrushi, 2013). The shoreline, which separates land from marine waters, is a dynamic feature that can simultaneously serve as an indicator of both coastal accretion and abrasion. (Nassar *et al.*, 2019). Shoreline change detection can be mapped through several approaches. Approaches using field survey techniques usually produce high accuracy measurements data, but this requires a long time, a lot of personnel, and high costs (Natesan *et al.*, 2013). Another costly approach is high-resolution aerial photography, which provides detailed topographic and shoreline data with high accuracy, although data acquisition may be periodic (Zhao *et al.*, 2008). While new approaches using Synthetic Aperture Radar (SAR) pictures and video, as well as Light Detection and Ranging (LiDAR) technology, can yield high-accuracy data, they are also expensive, which makes it more challenging to infer changes over time (Liu and Jezek, 2004; Nassar *et al.*, 2018).

Satellite imagery is also recommended as one of the data sources for shoreline detection (Boak and Turner, 2005). The usage of Landsat imagery, such as the Landsat-5 TM (Thematic Mapper), Landsat-7 ETM+ (Enhanced Thematic Mapper Plus), and Landsat-8 OLI (Operational Land Imager), for detecting changes in the coastline is increasing. They have been utilized in several coastal investigations across the world. To chart water bodies, several water indices have been created. In order to precisely identify and map land/water features from remotely sensed multi-spectral imaging. Shoreline positions were extracted using the Normalized Difference Water Index (NDWI), calculated as (Green – NIR) / (Green + NIR), with a threshold of 0.2 applied to distinguish land from water. Several studies have successfully used it to define coastlines in unpopulated areas using multi-temporal Landsat images. Urbanized beaches are problematic due to their lack of homogeneity and "noisiness." To address the issue of the noisy results brought on by urbanization, a switch was made from the near-infrared spectrum to the middle-infrared (Hui *et al.*, 2008; Xu, 2006).

In order to clearly define the border between land and water, satellite photography particularly digital data from remote sensing (RS) satellites with infrared spectral bands has grown in significance over the past few decades for the detection and mapping of coasts. Furthermore, utilizing satellite images as the basic data, RS data can be combined with Geographic Information Systems (GIS) as a helpful tool for analysis and extraction of more consistent and dependable information. (Kanwal *et al.*, 2020; Louati *et al.*, 2015; Mahapatra *et al.*, 2014). Since they are inexpensive and have a wide coverage, RS image-based techniques are being widely used to track changes in the coastline. Changes in the shoreline have been studied by numerous researchers, and the possible reasons for these changes have been identified and examined (Liu and Jezek, 2004; Nassar *et al.*, 2018).

One of the most crucial factors in coastal morphodynamical investigations and the detection of coastal erosion and deposition is shoreline calculation (Armenio *et al.*, 2019). As the boundary between land and ocean, shorelines are subject to constant change because of their dynamic environmental conditions. They change erratically in response to one or more environmental factors, such as morphological, climatic or geological factors (Mujabar and Chandrasekar, 2013). In order for stakeholders in coastal development projects to better mitigate the risk of coastal erosion and minimize social, physical, and financial losses, it is crucial to study shoreline change in order to comprehend the dynamics and evolution of coastal areas (Fuad and Fais, 2017). Given the unique geographic and climatic characteristics of Indonesia, few studies have carried out a thorough comparative investigation of shoreline spatial changes in the country over an extended period of time on national, island-wide and inter-provincial scales. Getting information on the spatial changes of the coastline at various scales in Indonesia as conducted by Sui *et al.* (2020) between 1990 and 2018, is a crucial approach for assessing the

ecological risks and development of coastal regions in multi-island nations, as well as for managing and protecting the coastline in a more scientific and sensible manner.

Numerous studies have examined the spatial and temporal change of coastlines using both qualitative and quantitative methods (Appeaning *et al.*, 2011; Maiti and Bhattacharya, 2009; Nassar *et al.*, 2019). The End Point Rate (EPR) technique combined with satellite imagery is an accurate and reliable method to calculate and analyze shoreline change (Sebat and Salloum, 2018). The Net Shoreline Movement (NSM) can be divided by the amount of time that has passed between the earliest and most recent coastline analyses to determine the EPR which is one of the calculations that requires only two shoreline dates to compute. There are many methods for analyzing shoreline change, but Linear Regression Rate (LRR) has the potential to analyze more than two shorelines (Burningham and French, 2017; Sheik and Chandrasekar, 2011). A least squares regression line is fitted to every coastline point along a specific transect in order to calculate LRR. LRR is obtained by looking at the friction of variance or corresponding r square value to which the regression is linked (Himmelstoss *et al.*, 2018).

Statistical rates of shoreline change are computed from time records of various coastline positions using the Digital Shoreline Analysis System (DSAS). The U.S. Geological Survey's Coastal Change Hazards project has benefited greatly from DSAS, which offers a reliable set of regression rates in a repeatable and consistent manner suitable for gathering vast volumes of data at various scales. In addition to providing rate of change information and arithmetic data that are crucial for controlling the consistency of the computation results, the software is intended to facilitate the process of estimating shoreline change (Mani Murali *et al.*, 2013). Additionally, DSAS can be used for broad applications that compute positional changes over time, including evaluating the changes in glacier bounds on historical aerial photos, river bank boundaries, or changes in land use and land cover (Thieler *et al.*, 2009). The three primary components of the method are establishing the baseline, producing orthogonal transactions (defined separations along the coast), and figuring out the rate of change, including amongst others the average rate, endpoint rate and, linear regression rate, utilizing certain models or techniques (Jonah *et al.*, 2015; Sheik and Chandrasekar, 2011).

Although the DSAS has been widely used due to its ability to assess shoreline and cliff dynamics effectively, it is not without limitations. For instance, DSAS relies heavily on the quality and temporal resolution of the input shoreline data, which can lead to inaccuracies when such data are sparse, inconsistent, or derived from heterogeneous sources (Himmelstoss *et al.*, 2018; Romine *et al.*, 2009). Additionally, the linear transect method employed by DSAS may oversimplify complex shoreline morphologies and ignore three-dimensional coastal processes (Pajak and Leatherman, 2002). Despite these limitations, DSAS remains a valuable tool for identifying morphodynamical forcing and enabling a comprehensive examination of the historical and temporal evolution of cliff geometry and coastline position alterations. (Nassar *et al.*, 2019). DSAS can be utilized to advance studies that focus on shoreline dynamics, shoreline erosion control, and vulnerability mitigation (Liew *et al.*, 2020). Sui *et al.* (2020) investigated shoreline changes and variations in coastal erosion and accretion in a long-term scenario using multi-temporal Landsat satellite images. Over the course of 28 years from 1990 to 2018, the overall trend observed along Indonesia's coastline during this period indicates an increase in the total coastline length. This includes a reduction in natural coastlines, a rise in artificial coastlines, and minimal alterations in the overall classification of secondary coastline categories (natural and artificial coastline). In Bali Province, Indonesia, high-resolution satellite imagery and the EPR method were utilized to analyze shoreline changes from 2016 to 2021. The study revealed significant coastal erosion linked to urban development and tidal influences. Similarly, an assessment of shoreline changes in Tamil Nadu, India, using Landsat data and the DSAS, identified patterns of erosion and accretion over a 30-year period, highlighting the impact of both natural and human-induced factors. In Costa Rica, long-term observations from 1986 to 2019 indicated that 50% of the Caribbean coastline experienced accretion, while 13% faced mild to severe erosion, underscoring the spatial variability of shoreline dynamics (Barrantes-Castillo and Ortega-Otárola, 2023; Hastuti *et al.*, 2024; Sekar *et al.*, 2024).

Most studies on shoreline change using DSAS focus on vertical shifts in shoreline distance to define abrasion and accretion processes (Nassar *et al.*, 2018; Quang *et al.*, 2021). These processes can be caused by natural factors (storm surge, wave intrusions, rising sea level, etc.) or human activities (coastal sand mining, river water conservation projects intercepting sediment, coastal engineering to enhance water power, beach vegetation damage). For instance, a study conducted in the coastal area of Jiangsu Province, China, utilized DSAS to analyze shoreline changes over a 45-year period, revealing that natural factors such as tidal currents and sediment deposition significantly influenced shoreline dynamics. Similarly, research in the Quang Nam Province of Vietnam employed DSAS

to assess shoreline evolution from 1990 to 2019, identifying that both natural factors like wave action and human activities such as coastal development contributed to the observed shoreline alterations (Quang *et al.*, 2021; Song *et al.*, 2021). This research, in addition to revealing changes in shoreline distance in the coastal area of the PT IWIP mining industry area, also provides analyses to determine changes in the extent of abrasion and accretion processes caused by mining area development activities. This research presents the ability to analyze shoreline changes using DSAS in a short time range (approximately five years) due to the pace of industrial area development. The purpose of this study is to analyze changes in the distance and extent of shoreline morphology changes along the coast of the IWIP industrial area using multi-temporal satellite imagery and classification techniques. The expected results of this research should provide useful information to achieve sustainable coastal management planning for mining activities in North Maluku province. In addition, this approach can be easily applied to other study areas with similar erosion/accretion problems.

2. Materials and Methods

2.1 Materials

The materials used in this study consist of satellite imagery and software tools for spatial and statistical analysis.

2.1.1 The equipments

The equipment used included a desktop computer with an Intel Core i7 processor, 32 GB RAM, and an NVIDIA GeForce GTX 1660 GPU for image processing and spatial analysis. ArcGIS 10.8 (Esri, USA) for shoreline digitization and spatial analysis, DSAS v5.0 (Digital Shoreline Analysis System) an official extension by USGS for ArcGIS, Microsoft Excel 2019 (Microsoft Corp., USA) for data tabulation, and QGIS 3.30 ‘s-Hertogenbosch (open-source GIS platform) for final visualizations.

2.1.2 The materials

The data used consisted of three series of Landsat 8 OLI satellite images, level 2A, path/row 109/60 acquired on July 27, 2018; October 26, 2022; and November 30, 2023. Images had less than 20% cloud content, and were, downloaded from the EarthExplorer portal (http://earthexplorer.usgs.gov). The imagery used has been terrain corrected, using ground control points and digital elevation models to achieve high geodetic accuracy. Its digital value is the surface object reflectance value (Level 2). Administrative boundary data, industrial zone data, and baseline shoreline from the Geospatial Information Agency (BIG), Indonesia.

2.1.3 Ethical approval

This study did not involve animal or human subjects and therefore did not require ethical approval.

2.2 Methods

This research was conducted along the coastline of the PT IWIP industrial area with a coastal length of approximately 18 km located around the mining area of PT IWIP, stretching from west to east between 127°55’31.75” - 128°2’30.63” longitude, and 0°27’31.97” - 0°28’40.19” latitude. Weda Bay has a steep, deep basin in the center of the bay that ranges in depth from 500 to 1700 meters. This topography may result in Weda Bay’s water masses having consistent physical characteristics distributed horizontally. Additionally, the depth increases toward the Halmahera Sea and decreases near the Southern and Eastern Halmahera shores (Abdul and Putri, 2013). Conditions in the coastal area prior to mining activities encompassed a residential area, sandy beach, and mangrove ecosystem. The analysis of shoreline changes was divided into seven zones based on activities in the coastal area: Lelilef village (Zone 1), Cekel airport (Zone 2), stockpile port (Zone 3), Company Mess (Zone 4), Logistics Port (Zone 5), coal stockpile (Zone 6) and Gemaf village (Zone 7). Administratively, the study area is included in the Central Weda District and North Weda District of Central Halmahera Regency, North Maluku Province (Figure 1).

2.3 Analysis Data

2.3.1 Shoreline extraction

Several standard methods of shoreline delineation have now been developed, to facilitate monitoring of shoreline changes using RS. The shoreline in this study is the waterline at the time of satellite image recording (Sui *et al.*, 2020). Shoreline extraction comparison techniques include digitization, threshold value utilization, and the squared error clustering method (SECM). Although the SECM method is the most effective, experts still frequently utilize more conventional techniques to define coastlines, such as computer interaction and human visual interpretation (Esmail *et al.*, 2019; Zhou *et al.*, 2019). Therefore, this study adopts these methods. Landsat satellite image data is presented through 543 false color (RGB) composites assisted by sharpening through digital value crunching, so that land and water objects can be visually separated and water and land boundaries digitized. The

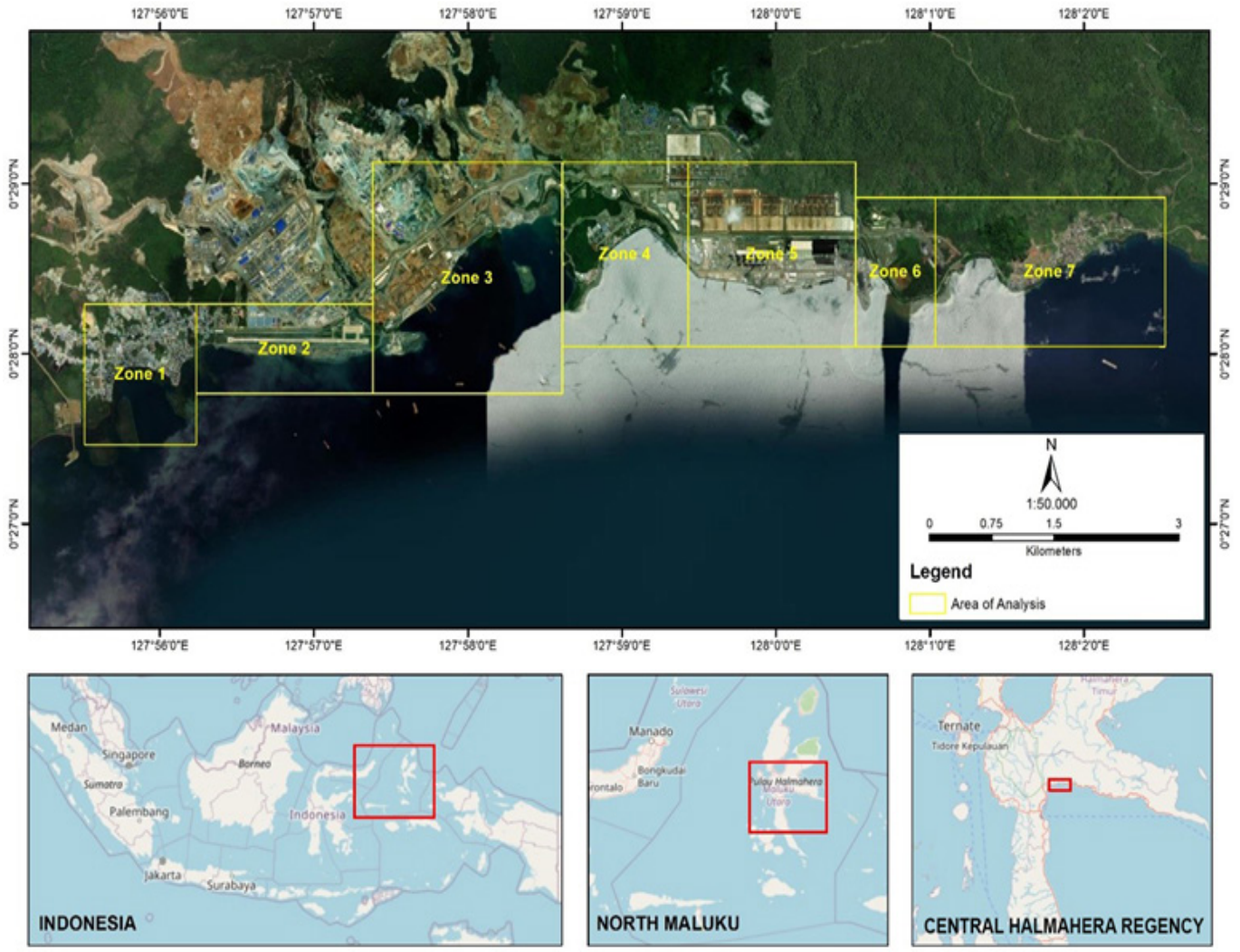

Figure 1. Map of the research location. Determined from Google Earth and Google Street Map base maps.

Coastline extraction technique begins with the use of land and sea area threshold values based on the NDWI algorithm modified by Xu (2006) with the equation:

MNDWI = (Green-SWIR) / (Green+SWIR).....(i)

Where :

MNDWI = the modified NDWI

SWIR = the mid-infrared band

which is band 6 of the Landsat 8 OLI image.

A sufficient positive threshold must be used to determine the water pixel values in order to classify the water-land boundary. For all land-water classes, the ideal threshold is zero (Fisher *et al.*, 2016). In order to automatically determine the border between land and water along the study area, this study employed the zero threshold (Quang *et al.*, 2021). The results of the shoreline extraction with the MNDWI algorithm were further improved using the digitization technique in the computer layer to obtain the shoreline in 2018, 2022 and 2023 (Figure 2).

2.3.2 Shoreline changes analysis

This study used the DSAS plug-in in the Environmental System Research Institute (ESRI) ArcGIS (Thieler *et al.*, 2009). NSM calculates the distance value between the oldest shoreline and the newest shoreline in meters. If the NSM value is less than zero then abrasion and if the NSM value is more than zero then accretion. EPR is calculated by dividing the distance of shoreline movement by the elapsed time between the oldest shoreline and the newest shoreline. The main advantage of EPR is its computational ease and the requirement of only two shoreline data series. The LRR computes long-term variations of the coastline change rate. Spaces among transects were noted based on the coastline change pattern alongside the baseline and transects (Kumar Das *et al.*, 2021).

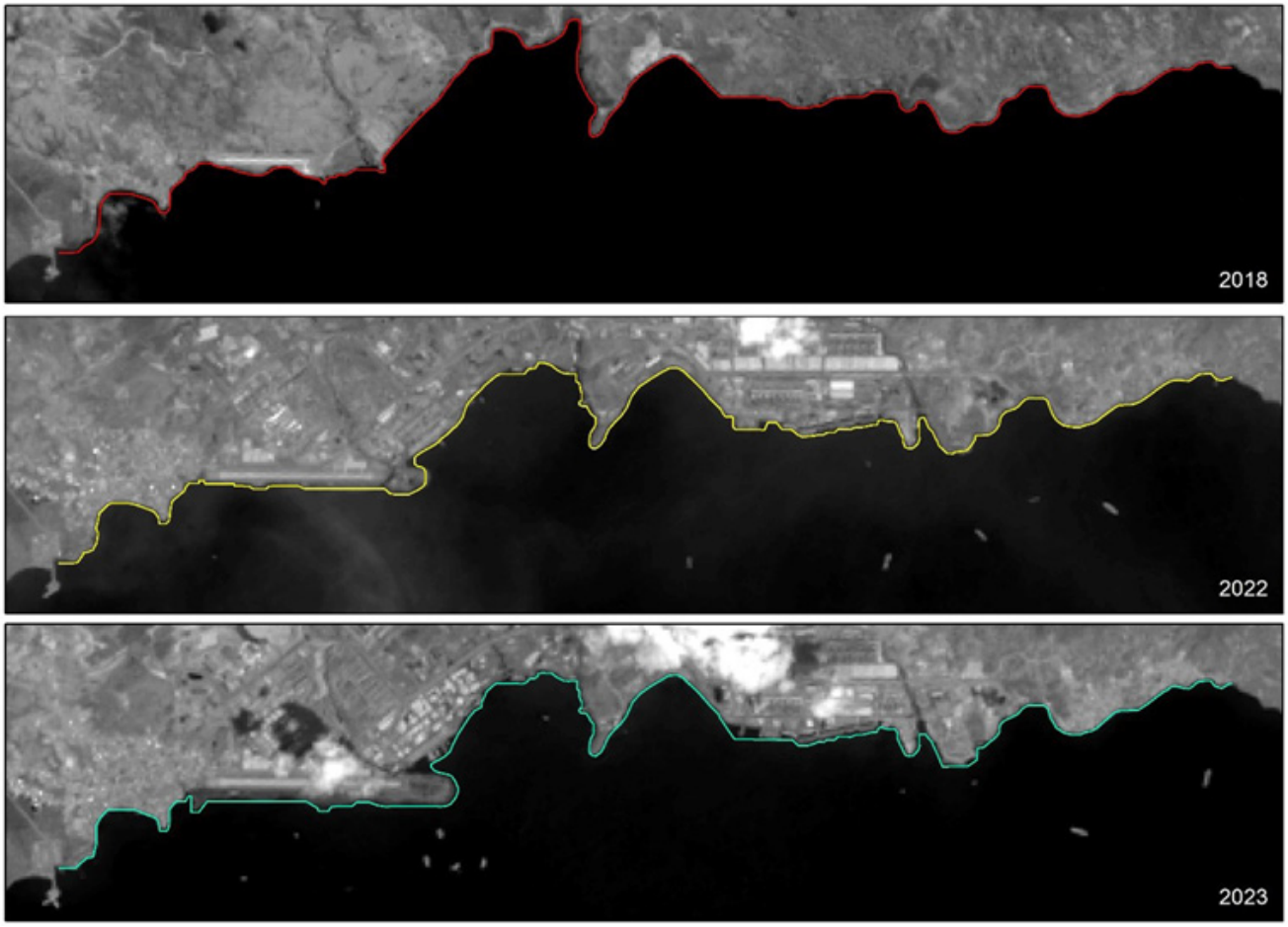

Figure 2. Shoreline extraction from Landsat imagery, showing the shoreline of the study area in 2018 (red line), 2022 (yellow line), and 2023 (green line).

The operation of DSAS begins with the determination of a baseline along and perpendicular to the shoreline that serves as the reference shoreline and the basis for calculating shoreline movement. Then, through a cast transect, DSAS intersects each shoreline to create measurement points these measurement points calculate the rate of shoreline change (Figure 3).

The DSAS applied to the shoreline of the PT IWIP mining industrial area is extracted and illustrated in (Figure 3). The transects shown represent the movement of the shoreline between year data series through the color of the lines categorized into different ranges. All transects change to a different color according to the range or linear distance that the position changes from the baseline at that location. Each transect represents the total shoreline movement value from the location where the transect is positioned. Positive values indicate accretion (i.e., movement of the landward edge towards the sea) and negative values indicate abrasion (the landward movement of the shoreline). The maximum distance between the baseline and the shoreline was set at 300 m from the 2018 shoreline and the distance between each transect was set at 40 m. Shoreline change rate was calculated using NSM to estimate the distance between the first and last shoreline. EPR was calculated by dividing the distance (m) separating two shorelines by the number of years between the dates of the two shorelines, and LRR was used to calculate the shoreline change rate statistically.

The rate of shoreline movement was also calculated based on the area in hectares. The resulting coastline was then merged with the administrative boundaries of Central Weda and North Weda Sub-districts (spatial features in the form of lines). The merged results were converted into polygon features, and the marker attributes of each polygon were added (the year coastline data source was recorded), then overlaid through union geoprocessing tools. All attribute markers were then merged in order of data year (2023, 2022, and 2018). The presence of 2023 as the last number in the merged row indicated accretion while 0 indicated abrasion. The analysis was then continued

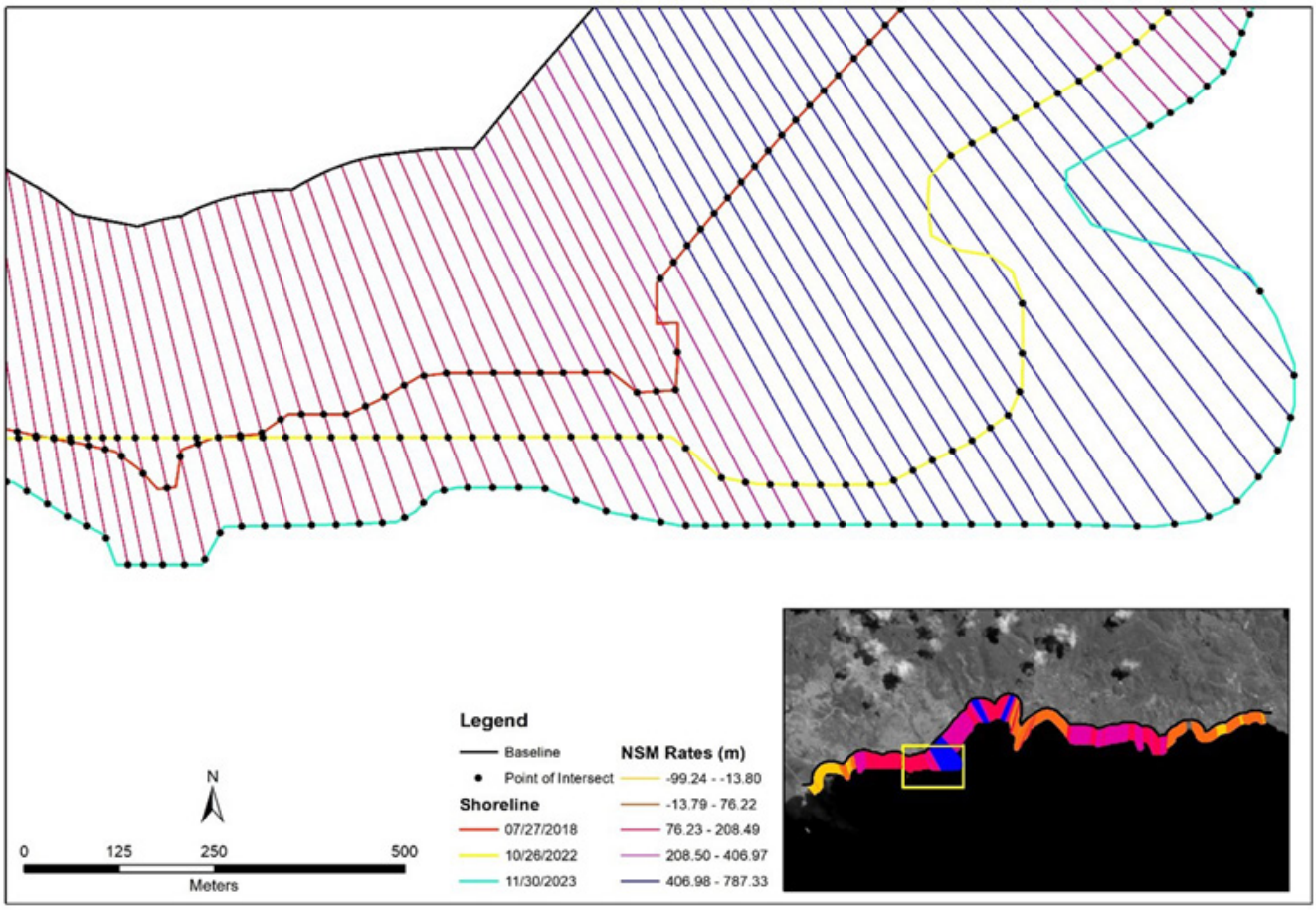

Figure 3. Shoreline change in the IWIP coastal area from 2018 to 2023. The coloured lines represent the shoreline positions at different time periods: the black line shows the baseline (pre-development shoreline), the red line shows the 2018 shoreline, the yellow line represents the 2022 shoreline, and the blue line shows the 2023 shoreline.

by calculating the extent of abrasion and accretion.

3. Results and Discussion

3.1 Results

3.1.1 Spatial pattern of accretion and abrasion

The results of the analysis to determine the process of abrasion and accretion show that in general the coast in the PT IWIP mining industrial area predominantly experienced accretion in the period 2018-2023 (Figure 4). Accretion mostly occurred in industrial area development zones such as Zone 2 (airport development), Zone 3 (stockpile port), Zone 4 (employee mess), Zone 5 (logistics port), and Zone 6 (coal stockpile), whereas Zones 1 and 7 (residential) and Zone 4 (employee mess) displayed lower levels of accretion. Across a total of 383 40 meter transects, the prevailing process was of accretion (71.28%), followed by abrasion (20.63%), with 8.09% fixed or unchanged. The addition of land area for the development of industrial areas for airport development, logistics ports, and coal stockpile in Zone 2, Zone 5 and Zone 6, resulted in 100% accretion in these zones. In the stockpile port area (Zone 3) and employee mess (Zone 4) the accretion process was 97.73% and 73.33% respectively. The abrasion process was most prevalent in Lelilef village settlement (Zone 1) at 94.00%, while substantial abrasion (38.24%) was also present in Gemaf village settlement (Zone 7). A small percentage of abrasion also occurred in Zone 3 and Zone 4 at 2.27% and 8.89% respectively.

The rate of shoreline changes in the PT IWIP mining industrial area for each year of observation was quite dynamic. Accretion and abrasion processes occurred throughout the year, but the accretion process dominated coastal dynamics. The longest accretion was found in the shorter 2022–2023-year range, at 594.64 meters long with an estimated accretion rate of 68.26 meters per year, while the maximum length (70.48 meters) of shoreline reduction (abrasion) was found in the longer 2018-2022 year range with an abrasion rate of 2.90 meters per year. If the observation duration is extended, the accretion rate decreases

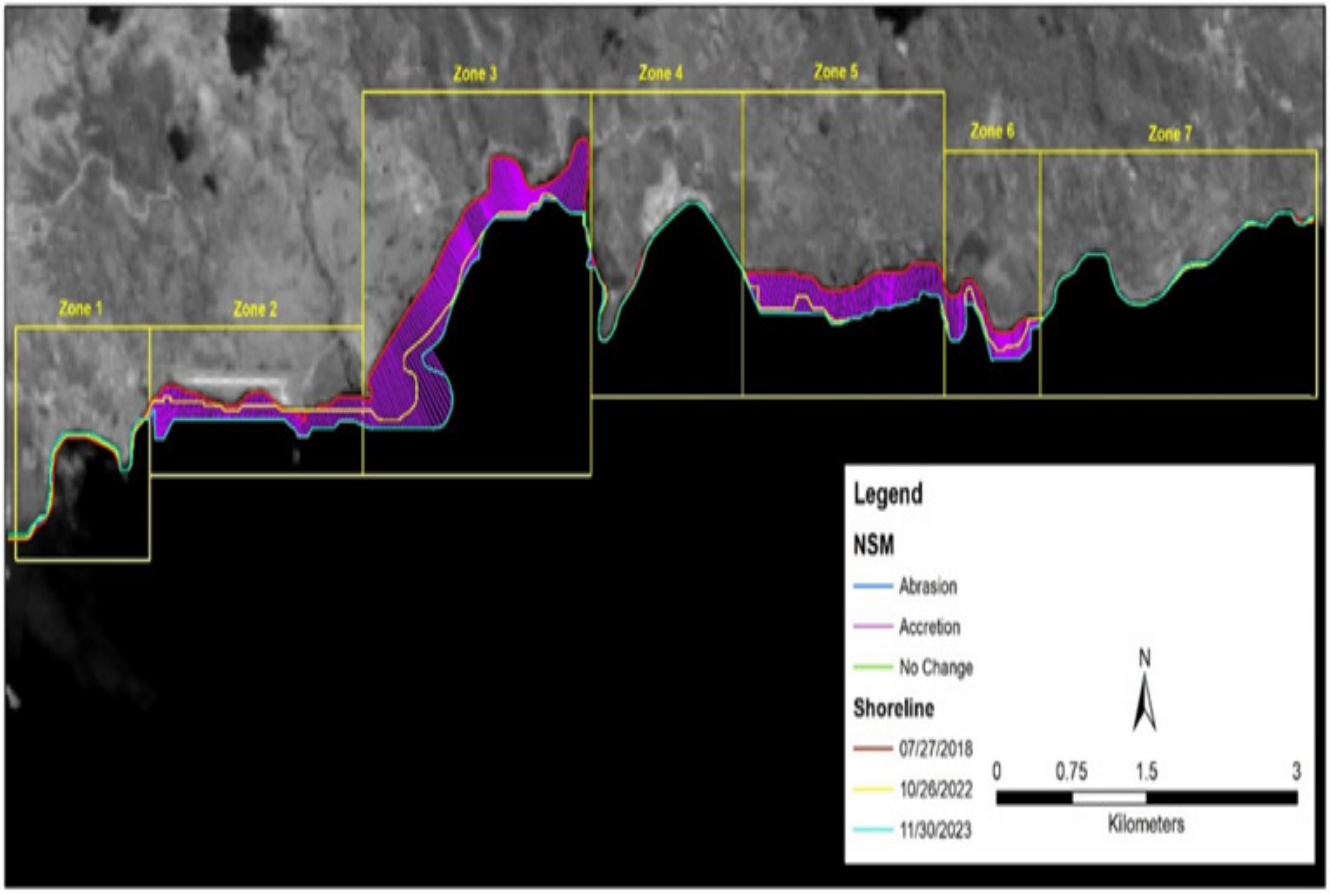

Figure 4. Analysis of shoreline changes to determine the occurrence of changes due to abrasion (blue line), accretion (purple line) and permanent or unchanged (green line) processes based on the NMS values in Zone 1 - Zone 7.

to 36.56 meters per year while the abrasion rate decreases to 4.10 meters per year (Table 1). The shoreline change in the 2018-2023 range was very dynamic, especially in the industrial development area of PT IWIP. Accretion of more than 400 meters took place in the stockpile port area (Zone 3) in the 2018-2022 period, and while the major location for abrasion was Lelilef village settlement area (Zone 1), the longest abrasion occurred in the airport development activities (Zone 2). In the 2022-2023 period with a shorter time than the 2018-2022 period, accretion occurred for more than 500 meters also in the stockpile port development area (Zone 3), while the longest abrasion occurred in the Lelilef village residential area (Zone 1) adjacent to the airport development area (Zone 2). The process of accretion and abrasion in the 2018-2023 timeframe is presented in Figure 5. As illustrated in Figure 5, the peaks in Zone 3 and Zone 2 (e.g., transects 110–140 and 50–90) reflect significant land accretion, especially between 2018 and 2022. In contrast, lower or negative values in Zones 1, 6, and 7 (e.g., transects 1–40, 320–350, and 360–379) suggest higher rates of abrasion or minimal accretion. This figure illustrates spatial variation in shoreline dynamics, highlighting more extensive coastal changes during the 2018-2022 period compared to 2022-2023.

3.1.2 Temporal trends and rates of shoreline change

The annual rate of shoreline changes in the PT IWIP mining industrial area during the period 2018-2023 was calculated using the EPR and LRR values (Figure 6). The positive and negative values of EPR and LRR shown in Figure 6 indicate accretion (positive values above the change line) and abrasion (negative values below the change line), respectively. Both methods show similar spatial patterns of shoreline change, although specific values differ. Peaks in Zones 2, 3, and 5 indicate areas of significant shoreline accretion, while Zones 1 and 7 are characterized by negative rates, indicating abrasion or retreat. The consistency in trend between LRR and EPR enhances the reliability of the observed spatial variability in shoreline dynamics and provides a robust comparison of accretion and erosion across different coastal segments. Overall, shoreline change in the PT IWIP

Table 1. Accretion and abrasion rates (meters) based on data recording time series.

Duration	Accretion (meters)		
	Maximum	Average	Per year
2018-2022	489.61	132.72	31.23
2022-2023	594.64	74.80	68.26
2018-2023	788.82	195.39	36.56
Duration	**Abrasion (meters)**		
	Maximum	**Average**	**Per year**
2018-2022	70.48	12.32	2.90
2022-2023	46.68	13.38	12.21
2018-2023	65.84	21.94	4.10

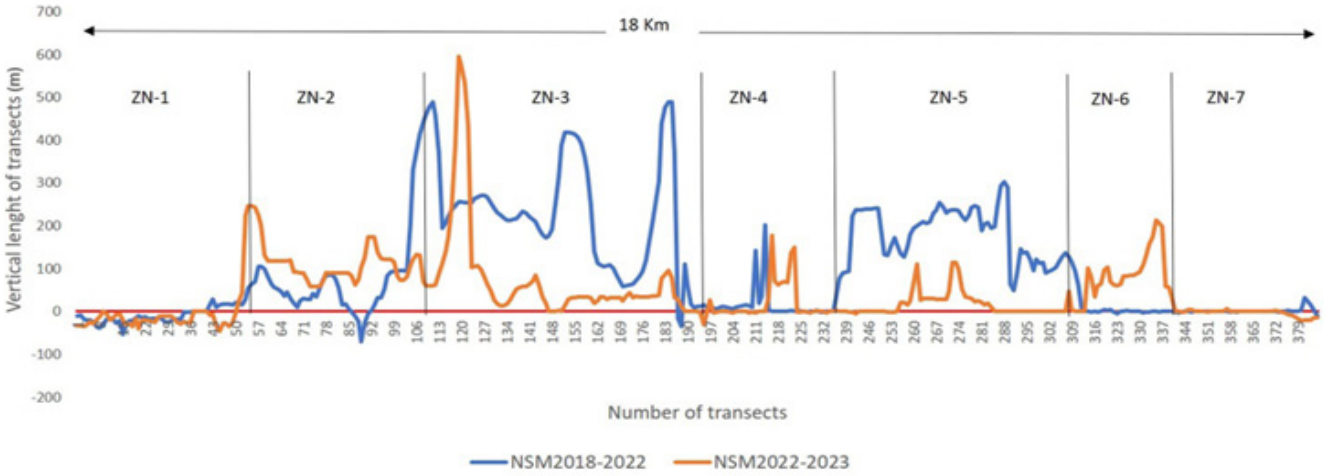

Figure 5. NSM along 379 transects divided into seven analysis zones (ZN-1 to ZN-7) over an 18 km coastline. The blue line represents NSM from 2018 to 2022, while the orange line shows NSM from 2022 to 2023. Positive values on the vertical axis indicate shoreline accretion (land gain), while negative values indicate shoreline retreat (erosion).

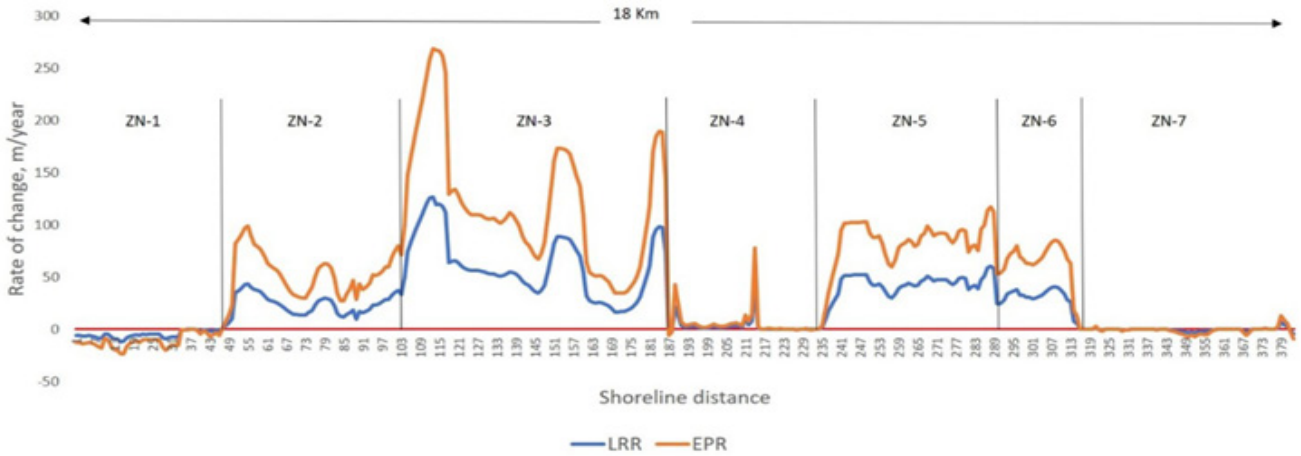

Figure 6. Rate of shoreline change (in m/year) along 379 transects across seven zones (ZN-1 to ZN-7) over an 18 km coastline, calculated using two statistical methods: LRR (blue line) and EPR (orange line).

mining industrial area within 5 years was characterized by accretion in the industrial development area, with a maximum rate of change of 147.58 meters/year and an average rate of change of 36.56 meters/year. The highest rate of change in coastlines characterized by abrasion was 12.32 meters/year, with an average rate of change of 4.11 meters/year at the settlement of Lelilef village in the western part and Gemaf village in the eastern part of the industrial area. Meanwhile, the rate of change based on the overall calculated statistical value of the shoreline illustrates a significant correlation between EPR and LRR with an R^2 (Figure 7), indicating no discernible difference between the EPR and LRR approaches for estimating the rate of shoreline change. The scatter plot shows a strong linear relationship ($R^2 = 0.9818$), indicating a high level of agreement between the two statistical methods. The regression equation ($y = 1.0218x + 0.1527$) suggests that EPR values are slightly higher than LRR values on average, but the overall trend is consistent. This result reinforces the reliability of both approaches in analyzing shoreline dynamics and supports the conclusions drawn from Figures 5 and 6 regarding patterns of coastal accretion and erosion. For abrasion, the maximum shoreline change rate was 12.32 m/year and 11.72 m/year, respectively for EPR and LRR.

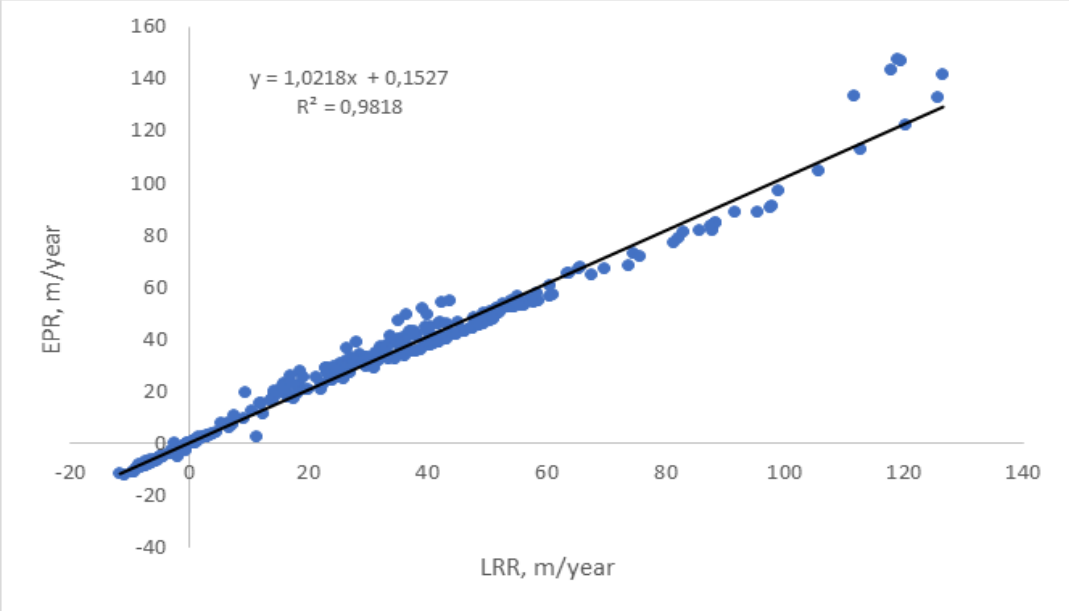

Figure 7. Correlation between shoreline change rates estimated using the LRR and EPR methods across 379 transects.

The results of the analysis of changes in the area of coastal dynamics within a period of 5 years (2018-2023) showed five models of change, namely: abrasion 2018-2022 and accretion 2022-2023, accretion 2018-2022 and abrasion 2022-2023, abrasion 2022-2023, accretion 2022-2023, and accretion 2023 (Table 2). The dynamic change in area from the process of abrasion followed by accretion vice versa (accretion then abrasion) or abrasion only, is influenced by water dynamics and industrial area development activities. This dynamic process of shoreline change, involving both erosion and accretion, was observed in nearly all monitoring zones, cumulatively affecting an area of approximately 7.64 hectares. Among these, the most significant abrasion was identified in the settlement area of Lelilef Village (Zone 1), which accounted for 2.58 hectares of the total affected area. Meanwhile, additional land area due to accretion was estimated to cover a total of 199.72 hectares. This included 138.74 hectares identified in the shoreline change model spanning 2022 to 2023, and a separate 60.98 hectares identified in the model based solely on changes occurring in 2023. This distinction helps to clarify that the two values represent results from different temporal models, rather than overlapping or cumulative measurements. Substantial accretion occurred in the industrial estate development areas of port stockpile (Zone 3) at 101.57 ha, port logistics (Zone 5) at 44.07 ha, airport (Zone 2) at 32.89 ha, and coal stockpile (Zone 6) at 18.89 ha. Minimal accretion was found in residential areas in the west, east, and employee mess (Zone 1,4, and 7) with an accretion area of 0.32 ha, 1.55 ha, and 0.43 ha, respectively (Figure 8). The map shows that substantial accretion (blue areas) predominantly occurred in industrial development zones, particularly in Zone 2, Zone 3, and Zone 5, suggesting significant land expansion associated with coastal reclamation and construction activities. Conversely,

Table 2. Area of change of abrasion and accretion in 2018-2023.

Changes	Zone 1	Zone 2	Zone 3	Zone 4	Zone 5	Zone 6	Zone 7	Total
Abrasion 2022, Accretion 2023	0.00	0.54	0.11	0.16	0.00	0.00	0.05	0.86
Abrasion 2022-2023	2.58		0.09	0.03			0.08	2.78
Accretion 2022, Abrasion 2023	2.86		0.25	0.00			0.89	4.00
Accretion 2022-2023	0.16	10.42	74.49	1.28	39.42	12.63	0.33	138.74
Accretion 2023	0.16	22.47	27.08	0.27	4.65	6.26	0.10	60.98

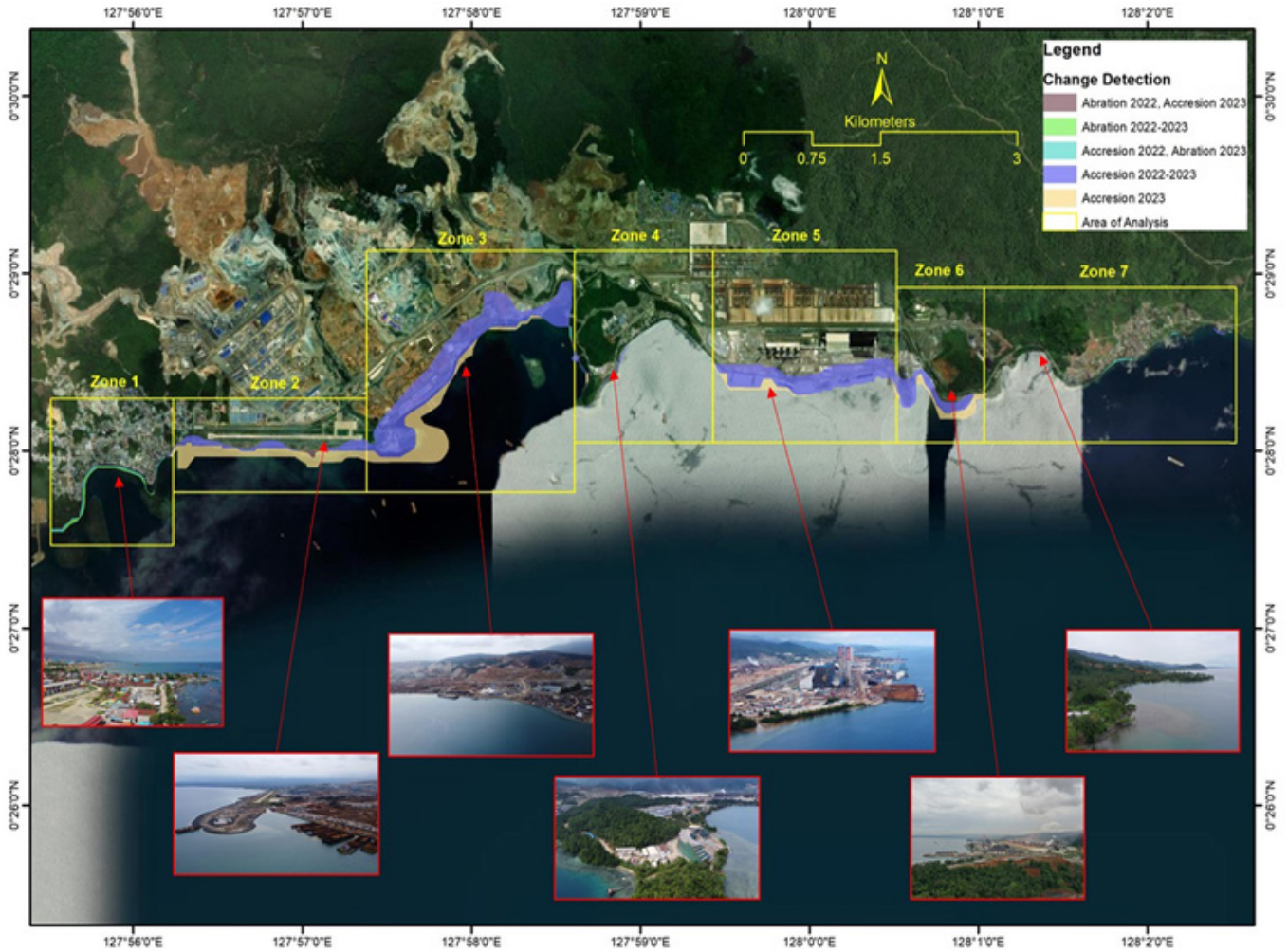

Figure 8. Location of shoreline changes indicating accretion and abrasion processes from 2018 to 2023.

areas of abrasion (brown and purple areas) were identified along the natural coastline in Zone 6 and Zone 7, where there has been limited or no coastal reinforcement. These spatial patterns highlight the strong correlation between anthropogenic activities and coastal morphology changes across the IWIP region. The accretion that occurred in the residential areas in the west and east was caused by the construction of coastal protection embankments, while the accretion in the employee mess area was caused by the development of accommodation facilities. The rate of expansion of the coastline towards the sea in the four-year period (2018-2022), reached 138.74 hectares or an average increase in area of 34.69 hectares/year. This was smaller than the rate of expansion of the coastline in the period 2022-2003. Although the change in area for

the 2022-2023 period lasted only one year, the shoreline area expansion rate reached 60.98 ha/year.

3.2 Discussion

3.2.1 Shoreline change patterns

This study used three methods to estimate the rate of shoreline change, namely NSM, EPR and LPR. These three methods are solid indicators for analyzing shoreline change. The results obtained show that a very large amount of shoreline change occurred in the period selected in this study. The results showed that the study area experienced substantial changes such as sea transgression and erosion during the observed period. The results are represented as positive and negative variables, which indicated accretion and erosion processes, respectively. When considering the data for the short period of this study of five years (2018-2023), it shows that the coastal area of the PT IWIP mining industrial area is moving towards the sea, where the beach turns into land more than the process of shoreline retreat. Based on the classification criteria for shoreline change put forward by Dey *et al.* (2021), this shows that the abrasion rate that occurs in the coastal area of the PT IWIP mining industrial area is categorized as moderate (-5 to -1), while the accretion rate is categorized as very high (>5).

Integration of RS and GIS technology is very useful for long term shoreline change studies using multispectral images with reasonable accuracy. Sui *et al.* (2020) found that, according to the results of the two periods, the total length of Indonesia's coastline has increased by 777.40 km over the past 28 years as a result of the comprehensive effects of human development and sea-land interaction. Of this, the natural coastline has decreased by 5994.52 km, the artificial coastline has increased by 6771.92 km, and the index of coastline utilization degree (ICUD) has increased by 16.74. The northern coast of the Maluku Islands, the southeast coast of Kalimantan, and the south coasts of Sumatra and Java have the biggest alterations to their artificial coastlines. According to the findings of Sui *et al.* (2020), Indonesia's natural coastline has made up over 70% of the country's entire coastline during the previous 28 years. This suggests that the country's coastline resources have not altered much and still have a vast amount of potential for development and use. The process of expanding the coastline towards or receding the coastline away from the sea will cause changes in the pattern of land and sea along the coastline. Land-to-sea advance or sea-to-land retreat are referred to as land invasion or transgression respectively. Land-to-sea advance in space is represented by an increase in land area, while sea-to-land retreat is represented by a decrease in land area. Changes in land area reflect the direction and magnitude of shoreline change. Conversely, changes in shoreline use also indicate the main driving factors and processes of land-sea pattern change.

The rate of shoreline changes in this study can be compared to research on the Peat Soil coast of Bengkalis Island, Riau Province, which was estimated over a period of 26 years from 1994 to 2014 (Sutikno *et al.*, 2017). The maximum abrasion rate on the Peat Soil coast of Bengkalis Island using the EPR and LRR methods had a value of 32.75 and 32.53 m/year, respectively, which is greater than the abrasion rate of 2.90 meters per year found in the current study. Conversely, the accretion rate observed in this study was much greater despite occurring in a shorter time span (5 years). The maximum rate of accretion on the Peat Soil coast of Bengkalis island by the EPR and LRR methods had a value of 39.21 and 44.52 m/year respectively, compared with 147.58 m/year and 126.53 m/year respectively in this study.

Research on shoreline changes using DSAS over a long period of time was also carried out in Tuban Regency, East Java Province, finding an average coastline retreat (EPR) of 15.24 m/year over 43 years from 1972 to 2015 in all of the Regency's coastal areas with an average shoreline movement (NSM) of 650.11 m. Abrasion and accretion of the coastline occurred in the coastal areas of Palang District from 1972 to 2000 displaying an average shoreline retreat of 15.73 m/year. The largest shoreline advance was found in the Fishery Harbor reclamation area. Shoreline retreat was also found in other sub-districts, namely Bancar, Tambakboyo, Tuban, and Jenu, with an average EPR of 14.55 m/year and an average NSM of 406.69 m. Shoreline progression and regression in all coastal areas of Tuban Regency were found in 2000-2013, 2013-2014, and 2014-2015 with an average EPR of 3.42, 17.45, and 30.56 m/year and an average NSM of 44.27, 17.6, and 22.69 m, respectively (Joesidawati and Suntoyo, 2016).

3.2.2 Coastal management implications

The overall trend of shoreline changes in Indonesia over 28 years between 1990 and 2018 has been an increase in the total length of the coastline, including a decrease in natural shorelines, an increase in artificial shorelines, and little change in the overall type of secondary category. In 1990, artificial shorelines in Indonesia were mostly distributed on the north coasts of Sumatra and Java, the west coast of Kalimantan, and Sulawesi. In 2018, the coverage of artificial shorelines across Sumatra Island reached 90%, and Java Island had also been fully developed. Changes in land-sea patterns had mainly occurred due

to the shrinkage of land into the sea, with 770.14 km^2 having expanded into the sea from 1990 to 2018. The most land expansion occurred in Riau Province, and the most seawater erosion was in West Java Province (Sui *et al.*, 2020).

As an archipelagic nation with more than 81,000 kilometers of coastline, Indonesia faces significant challenges in coastal zone management, particularly from human-driven activities such as coastal mining. These activities often result in shoreline erosion, sedimentation, and environmental degradation, leading to substantial changes in coastal morphology. RS technology has become an essential tool for effective monitoring and spatial planning in these dynamic areas. This study investigates shoreline changes in Central Halmahera Regency due to the expansion of mining activity zones. Using multispectral satellite imagery such as Landsat over a relatively short time period of five years, the analysis reveals a noticeable increase in coastal land area in certain locations. This shoreline growth is likely the result of activities such as land reclamation, artificial fill, or sediment deposition, closely linked to mining operations near the coast. While shoreline change is often associated with erosion, in this case, the process observed is accretion, where new land is formed, reshaping the natural coastline. These findings highlight how mining developments not only affect terrestrial ecosystems but also play a significant role in coastal dynamics. Continuous monitoring and data-driven planning are essential to ensure sustainable management of these rapidly changing coastal zones.

4. Conclusion

The results of this study show that DSAS based on geographic information systems has the ability to extract important information on the dynamics of shoreline change: both accretion (addition) and abrasion (reduction). The dynamics of shoreline change in the short period of time between 2018 and 2023 in the PT IWIP mining industrial area shows a very dynamic change process dominated by the line moving towards the sea, where the beach is converted into land more than the process of shoreline retreat. The abrasion rate is categorized as moderate, while the accretion rate is categorized as very high. This rate of change resulted in 199.72 hectares of additional land and 7.64 hectares of reduced land. The results of the spatio-temporal analysis of shoreline change within the overall PT IWIP industrial area showed that the industrial development area experienced accretion at a high to very high rate, while the residential area only experienced a very short period of erosion and then accretion. In addition, the results of temporal shoreline evolution show that the mechanism of shoreline change in the PT IWIP industrial area is predominantly caused by human activities (port and airport construction). This study's findings on the geographical dynamics of shoreline change will help coastal managers and planners to prioritize activities to address coastal environmental degradation. Knowing which regions are at risk of shoreline change allows local governments to adapt land-use planning and relocate populations and economic activities away from such locations.

Acknowledgement

The author would like to thank Mr Imran Taeran as the head of the Centre for Maritime Studies at Khairun University for his support of all research activities and facilities provided during the author's research in Central Halmahera Regency.

Authors' Contributions

The contribution of each author as follow: Nurhalis Wahidin; conceptualize, collected the data, analyzed data, and drafted the manuscript. Adi Noman Susanto, Irham and Muhammad Aris provided: conceptual ideas and critical revision of the article. Zulhan Arifin Harahap and Salnuddin: collected the data, analyzed the data, drafted the manuscript, and designed the Figures. All authors discussed the results and contributed to the final manuscript.

Conflict of Interest

The authors declare that they have no competing interests.

Declaration of Artificial Intelligence (AI)

The authors affirm that no artificial intelligence (AI) tools, services, or technologies were employed in the creation, editing, or refinement of this manuscript. All content presented is the result of the independent intellectual efforts of the author(s), ensuring originality and integrity.

Funding Information

This research did not receive any specific grant from funding agencies in the public, commercial, or not-for-profit sectors.

References

Abdul, B., & Putri, M. R. (2013). Water masscharacteristics Ofweda Bay, Halmahera Island, North

Maluku. *Jurnal Ilmu dan Teknologi Kelautan Tropis*, 5(2):365-376.

Al-Hatrushi, S. M. (2013). Monitoring of the shoreline change using remote sensing and GIS: A case study of Al Hawasnah tidal inlet, Al Batinah Coast, Sultanate of Oman. *Arabian Journal of Geosciences*, 6(5):1479-1484.

Appeaning, A. K., Jayson-Quashigah, P. N., & Kufogbe, S. (2011). Quantitative analysis of shoreline change using medium resolution satellite imagery in Keta, Ghana. *Marine Sciences*, 1(1):1-9.

Armenio, E., De Serio, F., Mossa, M., & Petrillo, A. F. (2019). Coastline evolution based on statistical analysis and modeling. *Natural Hazards and Earth System Sciences,* 19(9):1937-1953.

Barrantes-Castillo, G., & Ortega-Otárola, K. (2023). Coastal erosion and accretion on the Caribbean coastline of Costa Rica long-term observations. *Journal of South American Earth Sciences*, 127(7):1-14.

Boak, E. H., & Turner, I. L. (2005). Shoreline definition and detection: A review. *Journal of coastal research*, 21(4):688-703.

Burningham, H., & French, J. (2017). Understanding coastal change using shoreline trend analysis supported by cluster-based segmentation. *Geomorphology*, 282(2017):131-149.

Dey, M., Sakthivel, S. P., & Jena, B. (2021). A shoreline change detection (2012-2021) and forecasting using digital shoreline analysis system (DSAS) tool: A case study of Dahej Coast, Gulf of Khambhat, Gujarat, India. *Indonesian Journal of Geography,* 53(2):295-309.

Esmail, M., Mahmod, W. E., & Fath, H. (2019). Assessment and prediction of shoreline change using multi-temporal satellite images and statistics: Case study of Damietta Coast, Egypt. *Applied Ocean Research*, 82(2019):274-282.

Fisher, A., Flood, N., & Danaher, T. (2016). Comparing landsat water index methods for automated water classification in eastern Australia. *Remote Sensing of Environment*, 175(2016):167-182.

Fuad, M. A. Z., & Fais, D. A. M. (2017). Automatic detection of decadal shoreline change on Northern Coastal of Gresik, East Java – Indonesia. *IOP Conference Series*: *Earth and Environmental Science*, 98(1):1-11.

Hastuti, A. W., Nagai, M., Ismail, N. P., Priyono, B., Suniada, K. I., & Wijaya, A. (2024). Spatio-temporal analysis of shoreline change trends and adaptation in Bali Province, Indonesia. *Regional Studies in Marine Science*, 76(8):1-15.

Himmelstoss, E. A., Henderson, R. E., Kratzmann, M. G., & Farris, A. S. (2018). Digital shoreline analysis system (DSAS) version 5.0 user guide [Report](2018-1179). (Open-File Report, Issue. U. S. G. Survey.

Hui, F., Xu, B., Huang, H., Yu, Q., & Gong, P. (2008). Modelling spatial-temporal change of Poyang Lake using multitemporal Landsat imagery. *International Journal of Remote Sensing*, 29(20):5767-5784.

Joesidawati, M. I., & Suntoyo. (2016). Shoreline change in Tuban District, East Java using geospatial and digital shoreline analysis system (DSAS) techniques. *International Journal of Oceans and Oceanography*, 10(2):235-246.

Jonah, F. E., Adjei-Boateng, D., Agbo, N. W., Mensah, E. A., & Edziyie, R. E. (2015). Assessment of sand and stone mining along the coastline of Cape Coast, Ghana. *Annals of GIS*, 21(3):223-231.

Kanwal, S., Ding, X., Sajjad, M., & Abbas, S. (2020). Three decades of coastal changes in Sindh, Pakistan (1989–2018): A geospatial assessment. *Remote Sensing*, 12(1):1-24.

Kumar Das, S., Sajan, B., Ojha, C., & Soren, S. (2021). Shoreline change behavior study of Jambudwip Island of Indian Sundarban using DSAS model. *The Egyptian Journal of Remote Sensing and Space Science*, 24(2):961-970.

Liew, M., Xiao, M., Jones, B. M., Farquharson, L. M., & Romanovsky, V. E. (2020). Prevention and control measures for coastal erosion in northern high-latitude communities: A systematic review based on Alaskan case studies. *Environmental Research Letters*, 15(9):1-22.

Liu, H., & Jezek, K. C. (2004). Automated extraction of coastline from satellite imagery by integrating canny edge detection and locally adaptive thresholding methods. *International Journal of Remote Sensing*, 25(5):937-958.

Louati, M., Saïdi, H., & Zargouni, F. (2015). Shoreline change assessment using remote sensing and GIS techniques: A case study of the Medjerda Delta Coast, Tunisia. *Arabian Journal of Geosciences*, 8(6):4239-4255.

Mahapatra, M., Ratheesh, R., & Rajawat, A. S. (2014). Shoreline change analysis along the coast of South Gujarat, India, using digital shoreline analysis system. *Journal of the Indian Society of Remote Sensing*, 42(4):869-876.

Maiti, S., & Bhattacharya, A. K. (2009). Shoreline change analysis and its application to prediction: A remote sensing and statistics based approach. *Marine Geology*, 257(1):11-23.

Mani Murali, R., Ankita, M., Amrita, S., & Vethamony, P. (2013). Coastal vulnerability assessment of Puducherry coast, India, using the analytical hierarchical process. *Natural Hazards and Earth System Sciences,* 13(12):3291-3311.

Mujabar, P. S., & Chandrasekar, N. (2013). Shoreline change analysis along the coast between Kanyakumari and Tuticorin of India using remote sensing and GIS. *Arabian Journal of Geosciences*, 6(3):647-664.

Nassar, K., Fath, H., Mahmod, W. E., Masria, A., Nadaoka, K., & Negm, A. (2018). Automatic detection of shoreline change: Case of North Sinai Coast, Egypt. *Journal of Coastal Conservation*, 22(6):1057-1083.

Nassar, K., Mahmod, W. E., Fath, H., Masria, A., Nadaoka, K., & Negm, A. (2019). Shoreline change detection using DSAS technique: Case of North Sinai Coast, Egypt. *Marine Georesources & Geotechnology*, 37(1):81-95.

Natesan, U., Thulasiraman, N., Deepthi, K., & Kathiravan, K. (2013). Shoreline change analysis of Vedaranyam coast, Tamil Nadu, India. *Environ Monit Assess*, 185(6):5099-5109.

Pajak, M. J., & Leatherman, S. P. (2002). The high water line as shoreline indicator. *Journal of coastal research*, 18(2):329-337.

Quang, D., Ngan, V., Ho, T., Viet, N., Tinh, N., & Tanaka, H. (2021). Long-term shoreline evolution using DSAS technique: A case study of Quang Nam Province, Vietnam. *Journal of Marine Science and Engineering*, 9(10):1-18.

Romine, B., Fletcher, C., Frazer, N., Genz, A., Barbee, M., & Lim, S.-C. (2009). Historical shoreline change, Southeast Oahu, Hawaii; Applying polynomial models to calculate shoreline change rates. *Journal of Coastal Research Journal of Coastal Research*, 25(2):1236-1253.

Sebat, M., & Salloum, J. (2018). Estimate the rate of shoreline change using the statistical analysis technique (EPR). *Bit Numerical Mathematics*, 1(2018):59-65.

Sekar, L. G., Androws, X., Annaidasan, K., Kumar, A., Kannan, R., Muthusankar, G., & Balasubramani, K. (2024). Assessment of shoreline changes and associated erosion and accretion pattern in coastal watersheds of Tamil Nadu, India. *Natural Hazards Research*, 4(2):231-238.

Sheik, M., & Chandrasekar. (2011). A shoreline change analysis along the coast between Kanyakumari and Tuticorin, India, using digital shoreline analysis system. *Geo-Spatial Information Science*, 14(4):282-293.

Song, Y., Shen, Y., Xie, R., & Li, J. (2021). A DSAS-based study of central shoreline change in Jiangsu over 45 years. *Anthropocene Coasts*, 4(1):115-128.

Sui, L., Wang, J., Yang, X., & Wang, Z. (2020). Spatial-temporal characteristics of coastline changes in Indonesia from 1990 to 2018. *Sustainability*, 12(8):1-28.

Sutikno, S., Sandhyavitri, A., Haidar, M., & Yamamoto, K. (2017). Shoreline change analysis of Peat Soil Beach in Bengkalis Island based on GIS and RS. *International journal of engineering and technology*, 9(3):233-238.

Thieler, E. R., Himmelstoss, E. A., Zichichi, J. L., & Ergul, A. (2009). The digital shoreline analysis system (DSAS) Version 4.0 - An ArcGIS extension for calculating shoreline change [Report](2008-1278). (Open-File Report, Issue. U. S. G. Survey.

Xu, H. (2006). Modification of normalised difference water index (NDWI) to enhance open water features in remotely sensed imagery. *International Journal of Remote Sensing*, 27(14):3025-3033.

Zhao, B., Guo, H., Yan, Y., Wang, Q., & Li, B. (2008). A simple waterline approach for tidelands using multi-temporal satellite images: A case study in the Yangtze Delta. *Estuarine, Coastal and Shelf Science*, 77(1):134-142.

Zhou, M., Wu, M., Zhang, G., Zhao, L., Hou, X., & Yang, Y. (2019). Analysis of coastal zone data of Northern Yantai collected by remote sensing from 1990 to 2018. *Applied Sciences*, 9(20):1-20.